Characteristics of Airborne and Spaceborne Height Models

Karsten Jacobsen

Leibniz University Hannover, Institute of Photogrammetry and Geoinformation, Germany; jacobsen@ipi.uni-hannover.de

Abstract. Nearly worldwide covering height models are based on optical or synthetic aperture radar (SAR) imagery. They describe a digital surface model (DSM) with points on top of buildings and vegetation. Only with P- or L-band radar the vegetation can be penetrated. The accuracy and details mainly depend upon the ground sampling distance (GSD) of the images. DSM based on SAR have some problems with lay over, especially in mountainous, but also in build up areas. With the very high resolution space images overlap to aerial images exist and the use of aerial or space imagery is just a question of access and economy. For very detailed height models aerial images or LiDAR can be used. In any case the height models have to be filtered if a digital terrain model (DTM) with the height of the bare ground shall be generated. Such a filtering is possible in build up areas, including always some points on bare ground, but special filters are required for filtering very large buildings or vegetation areas in LiDAR. An overview about the height models and the filtering to DTM will be given.

Keywords. Spaceborne, airborne, optical images, SAR, DHM generation, accuracy, filtering

1. Introduction

Digital height models (DHM) are basic information about a terrain. They can be generated based on optical stereo pairs, synthetic aperture radar or LiDAR depending on the requirements and conditions. Today the very high resolution (vhr) optical space images have an overlapping range of ground resolution to aerial images, so the selection of aerial, space images or even LiDAR is just a question of economy and access to the data. If a whole country shall be covered with optical images of 0.5m ground sampling distance (GSD), in most cases digital aerial images are less expensive as space images, but in some countries the use of aerial images is restricted while this is not the case for space images. The acquisition of LiDAR data is more time consuming; that means also more expensive, as the acquisition of LiDAR data, limited to a smaller field of view to reduce viewing shadows and to a lower flying elevation for having a satisfying point density. The covering of large parts of the world with height models is not realistic with vhr optical stereo pairs, this is only possible with optical stereo satellites as ASTER with 15m GSD, SPOT-5 HRS with 5m GSD, Cartosat-1 with 2,5m GSD and with Zyuan-3 with 3.2m GSD or with SAR-images, especially with interferometric constellation as with the Shuttle Radar Topography Mission (SRTM) or the TanDEM-X constellation. Of course with the high resolution aerial images or with LiDAR higher accuracy can be reached as with space data, but only for limited areas. Nevertheless with exception of the accuracy the characteristics of DHM based on aerial images is similar as for optical space images. Only with long wavelength radar – L- or P-band – the vegetation can be penetrated as for LiDAR in case of not too dense canopy. All other data sources will lead to digital surface models (DSM), nevertheless in any case buildings will be included in the DHM

2. LiDAR

Neighbored points of a DHM determined by matching of optical images are correlated because of overlapping windows of area based matching, but also with pixel based matching, as e.g. semi global matching, neighbored points are depending upon the optimal path. Also in the case of radar a continuous surface is generated. This is different for LiDAR where points of the point cloud are independent with the exception of the orientation. If the laser beam hits a bird in the sky, the neighbored point may be on the ground, not affected by the isolated elevated point. Beside application for forest reason, especially height models based on the first and the last pulse are important. The first pulse represents a DSM while with the last pulse the tendency goes to a digital terrain model (DTM) with points on the bare ground. Of course also buildings are included in the last pulse point cloud, but they can be eliminated by filtering. Nevertheless in vegetation not all last pulses will reach the ground, requiring also a filtering. If overlapping LiDAR strips are compared, the not filtered last pulse DHM shows discrepancies in vegetation, but also at building boundaries. In one strip a point may be located on the roof overhang, while in the overlapping strip the point with similar horizontal location may be located on the ground or even the façade (figure 1 left and right in upper part with points on facade).

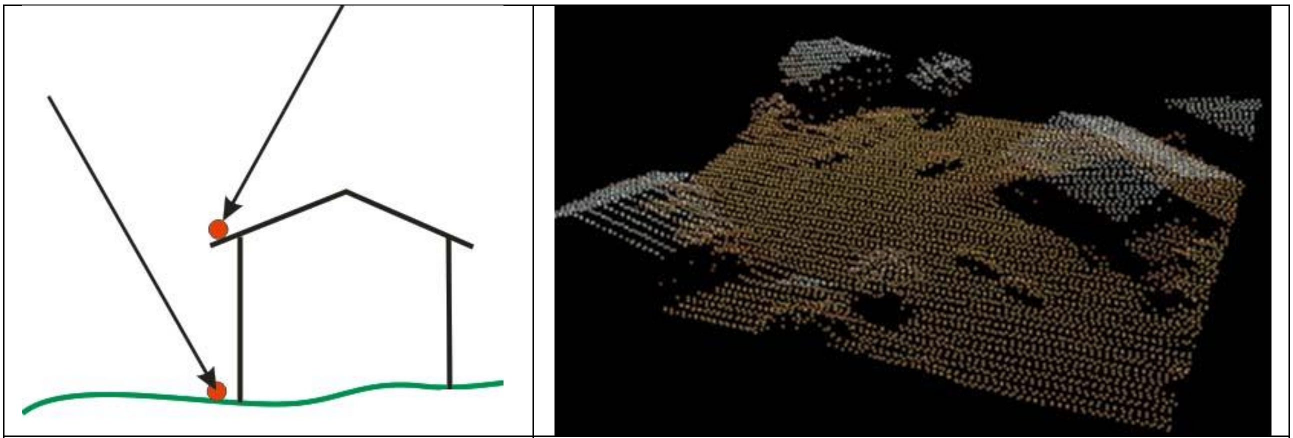

Location of points in overlapping area	Point cloud

Figure 1. Location of LiDAR-points

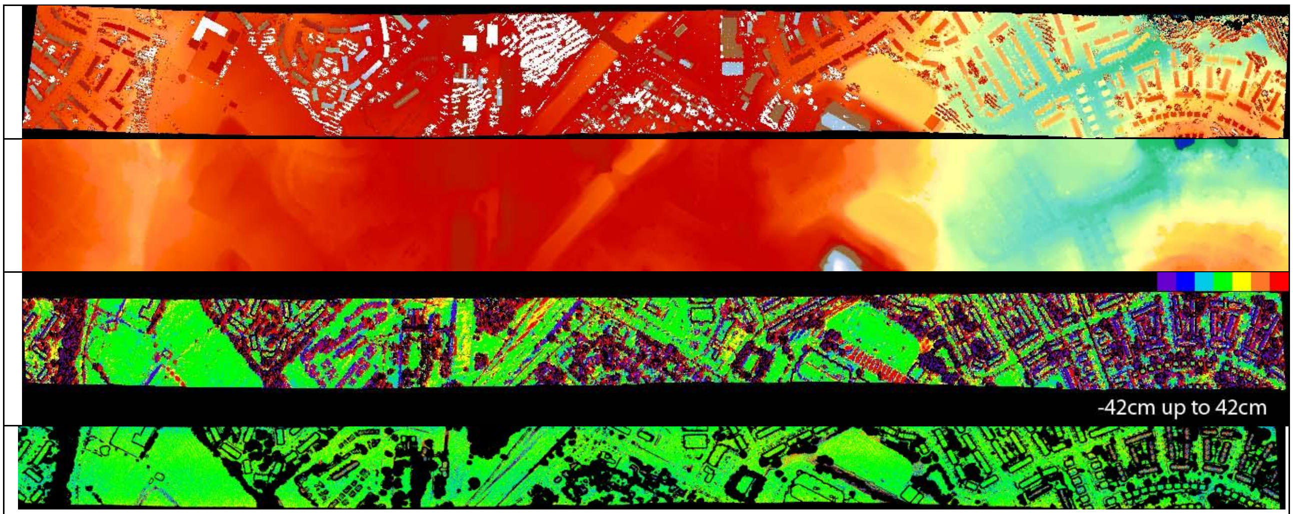

-42cm up to 42cm

Figure 2. From above: LiDAR DSM, LiDAR DTM, difference of overlapping strips, difference after vegetation filtering and rotation

Figure 2 upper shows a typical DSM as color coded LiDAR strip, the second image from above shows a typical DTM, generated by filtering and interpolation of the LiDAR strip above with Hannover program RASCOR (Day et al. 2002, Passini et al. 2013). In this case approximately 50% of the points have been eliminated, being located mainly on vegetation and buildings. If overlapping LiDAR strips are compared, the height discrepancies shown color coded in figure 2, 3rd from above, indicate large discrepancies in vegetation areas and at building corners. The standard deviation of the height (SZ) discrepancies is 0.24m, while the normalized median absolute deviation (NMAD) is below with 0.12m. NMAD is the median multiplied with a factor 1.482 to reach a probability level of 68% - the same as the standard deviation under condition of normal distributed discrepancies. If SZ and NMAD are showing such differences, the discrepancies are not normal distributed as it can be seen in figure 3 left. Figure 3 shows the frequency distribution of the discrepancies in blue and the overlaid normal distribution based on SZ in red and based on NMAD in brown. The deviation from normal distribution is caused by the high number of large discrepancies with 12.3% exceeding 0.5m. Large discrepancies are affecting the standard deviation strongly, but not as much the NMAD, so the normal distribution based on NMAD is not far away from the major part of the frequency distribution. Figure 3, right, shows the same after vegetation filter, here 0.09m SZ and 0.07m NMAD has been reached. Now the standard deviation based on NMAD and also SZ fit not bad to the major part of the frequency distribution. This is typical for all height models whether they are from LiDAR, airborne or spaceborne optical or radar images.

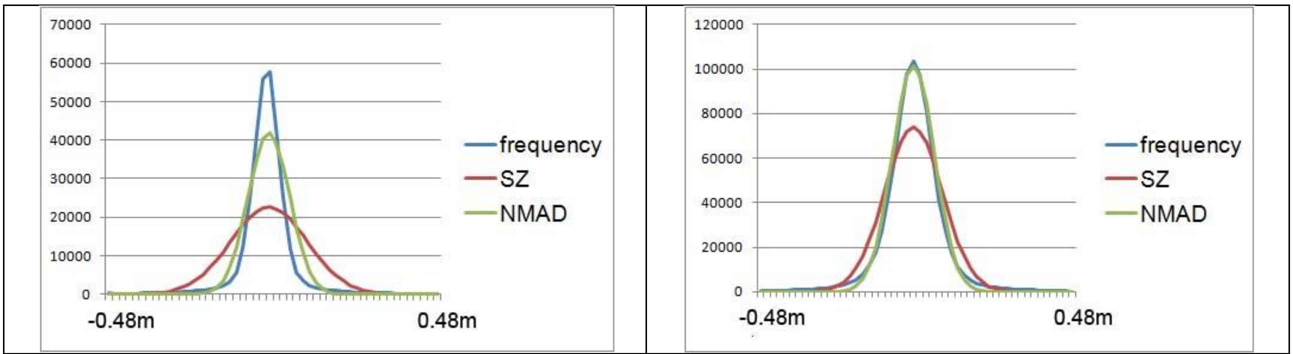

difference original LiDAR data of overlapping strips	same data after vegetation filter and rotation

Figure 3. Frequency distribution with overlaid normal distribution based on NMAD and SZ

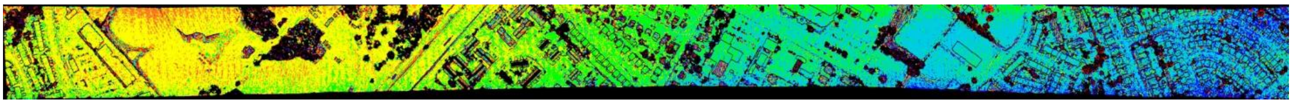

Figure 4. Color coded height differences of overlapping LiDAR strips after vegetation filter

Not all overlapping LiDAR strips are fitting well together as shown in figure 2. Figure 4 indicates clear systematic differences across and along flight direction. Such systematic errors, caused by the direct sensor orientation, are typical for LiDAR. In this case in flight direction 0.0022°, corresponding to 10.3cm over whole range, and across 0.0472° difference, corresponding to 2cm, in orientation exist. If the full system accuracy of LiDAR shall be reached, a block adjustment of the LiDAR strips is required including height control areas. In a project in the area of Istanbul using a Riegl LSM-Q680i after block adjustment with 16 check points located on a tennis court a standard deviation of 3cm has been reached. In this case the absolute accuracy was identical to the relative, this usually cannot be expected, but it shows the possible relative accuracy which can be reached on a perfect plane. Usually the point definition is not as good and the height variation within the footprint influences the accuracy.

3. Airborne height determination

In the same area as the LiDAR flight shown above, a photo flight with the UltraCam Eagle of Keystone Aerial Surveys with 5cm ground sampling distance (GSD) has been made. By bundle block adjustment with targeted ground control points at independent check points root mean square Z-differences of 5.6cm has been reached. This system accuracy of approximately one GSD is typical for optical aerial and space images. Of course the system accuracy is not identical to the determination quality of a height model which depends upon the object contrast and the point definition in object space. So with the Socet Set NGATE matching program as well as with Correlator 3D height models with 50 cm spacing were extracted.

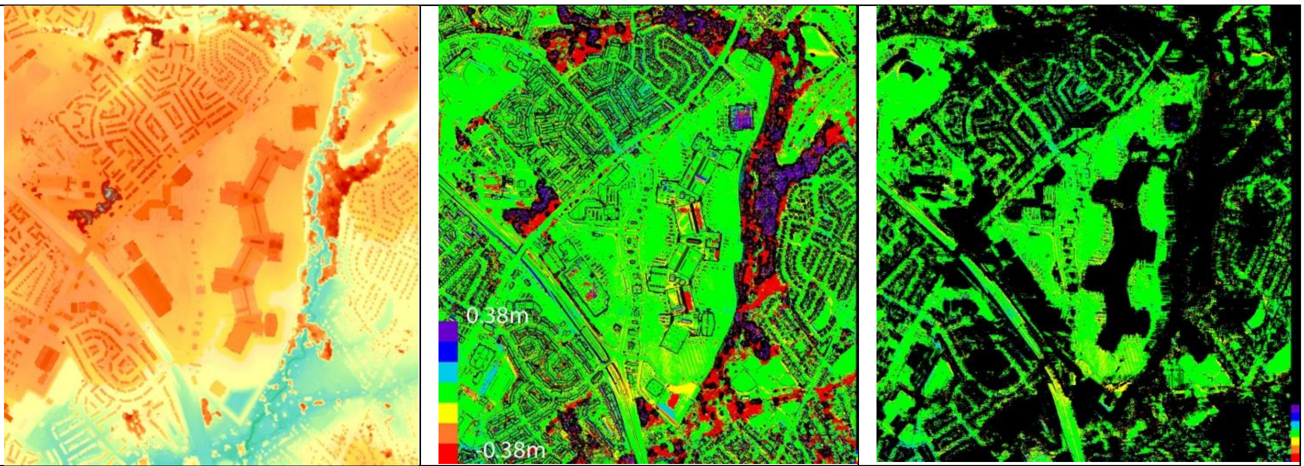

Color coded DSM	Differences NGATE – Correlator 3D DSM	Differences NGATE – Correlator 3D DTM

Figure 5. Comparison height models from NGATE and from Correlator 3D

The test area is built up with usual houses and a large shopping mall. The housing area and some other parts are covered by vegetation (figure 5 left). If the directly generated DSM are compared, larger differences can be seen mainly in the vegetation areas, but also on the roof of the shopping mall with low contrast larger discrepancies exist (figure 5, center). If the area is filtered from DSM to DTM, the larger discrepancies between the DTM from NGATE and from Correlator 3D disappears (figure 5, right).

Table 1. Comparison height model from NGATE and from Correlator 3D

Differences NGATE – Correlator 3D	SZ	SZ as F(slope)	NMAD	NMAD as F(slope)
DSM	24cm	10cm + 121cm∗tanα	10cm	7cm + 69cm∗tanα
DTM (filtered)	19cm	8cm + 144cm∗tanα	18cm	6cm + 116cm∗tanα

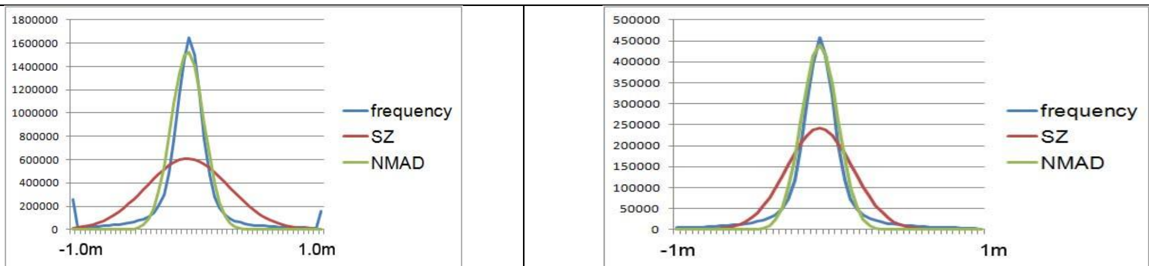

DSM	DTM filtered from DSM

Figure 6. Frequency distribution of height model differences NGATE – Correlator 3D

The standard deviation and the NMAD as well as the frequency distribution of the differences between the height models from NGATE and from Correlator 3D show the problems of the height models based on different image combinations. As usual SZ is larger as NMAD caused by the higher number of larger discrepancies, shown also in figure 6 left. The discrepancies even would be larger if not a threshold limit of 1.0m had been used for accepted differences. By filtering the discrepancies are getting slightly smaller and even smaller for flat areas. The differences of the original and also the filtered data are clearly depending upon the terrain inclination (table 2). The NMAD for the flat terrain with 6cm is in the range of the GSD.

Table 2. DHM from matched digital aerial images against LiDAR reference - SZ, NMAD and as function of the terrain inclination with the slope α

	SZ	NMAD	LE90	LE95
NGATE original	14.4cm 12.2cm + 50cm∗tan α	16.1cm 9.7cm + 10cm∗tan α	25.5cm (SZ∗1.51)	32.2cm (SZ∗2.38)
NGATE filtered	11.8cm 10.4cm + 32cm∗tan α	12.9cm 8.7cm + 15cm∗tan α	20.3cm (SZ∗1.57)	25.6cm (SZ∗1.98)
Correlator 3D original	14.1cm 10.4cm + 94cm∗tan α	15.5cm 8.3cm + 34cm∗tan α	23.5cm (SZ∗1.63)	31.0cm (SZ∗2.15)
Correlator 3D filtered	12.5cm 10.4cm + 55cm∗tan α	13.9cm 8.7cm + 34cm∗tan α	20.2cm (SZ∗1.56)	25.7cm (SZ∗1.99)

This is a typical result for aerial images. Of course the discrepancies of the DHM based on aerial images against LiDAR is larger as the system accuracy, which is in the range of 1.0 GSD, but if height models are compared, the object structure as caused by vegetation has to be respected. After filtering the DHM from aerial images the discrepancies against the LiDAR heights are getting smaller and finally for not inclined areas the NMAD is in the range of 8cm to 9cm what can be accepted.

Large area covering height models also can be generated by airborne Interferometric Synthetic Aperture Radar (InSAR) as this has been made by Intermap Technologies for NEXTMap covering Western Europe, the main part of the USA, parts of Indonesia and Australia as well as Malaysia and some other parts taken from a height of 10.4km. The NEXTMap height model has a point spacing of 5m. With the used X-band vegetation cannot be penetrated, so originally also a DSM was generated. SAR has the general problem of foreshortening and lay over, causing problems of determining object heights in areas with stronger inclination against view direction. By this reason the specification of the vertical accuracy is as follows: for 40% of the area < 1m LE90 (SZ<0.60m), for another 40% of the area 1m up to 3m LE90 (SZ=0.60 up to 1.8m) and for the final 20% of the area >3m LE90 (SZ >1.8m). This wide range of accuracy is typical for InSAR with the highest accuracy in open and not so steep areas and limited accuracy in build up areas, forest and steep mountains.

4. Spaceborne height determination

Height models based of spaceborne information may use optical or SAR-data. The images used for a stereo model should come from the same orbit to avoid changes in the object space as changed shadows. With the today very flexible satellites it is not a problem to take the images approximately within one minute by rotating the satellite. Especially both WorldView satellites as well as Pleiades rotate very fast, allowing even to take other images within between. In the case of InSAR a configuration of two satellites e.g. the TanDEM-X configuration or the SRTM-mission with two antennas should be preferred to avoid de-correlation. If the images are not from such a configuration, the DHM-generation should be based on radargrammetry.

Worldwide DHM coverage by optical images is only possible with stereo satellites having ground resolution starting at 2.5m and several years of data acquisition as with Cartosat-1 (2.5m

GSD), SPOT-5 HRS (5m HSD in orbit direction), ASTER (15m GSD) and Ziyuan-3 (3.5m). With very high resolution satellites (≤1m GSD) only local up to regional coverage is possible. For reaching highest absolute accuracy ground control points (GCP) have to be used. If no GCP are available, the absolute orientation accuracy is limited to the accuracy of the direct sensor orientation (table 3); nevertheless this does not influence the relative accuracy within a stereo scene.

Table 3. Accuracy of direct sensor orientation without GCP

Sensor	SX = SY	CE90
IKONOS	7m	15m
QuickBird	9m	23m
Orbview-3	12m	25m
WorldView-1	2m	5m
WorldView-2	2m	5m
GeoEye-1	2m	5m
Pleiades	4m	8.5m
Cartosat-1 / with in-flight calibration	200m / 30m (Euromap 7m)	(Euromap 15m)
KOMPSAT-2	37m	80m

If the accuracy of the direct sensor orientation is not satisfying a DHM can be generated just with improved relative orientation and this DHM can be fitted to a better reference as it is available for example with the SRTM height model or in 2014 with the even more precise TanDEM-X Global DEM. This for example is done for EURO-MAPS 3D to improve the location of Cartosat-1 DHM.

The accuracy of height models based on optical images is dominated by the GSD. The base to height relation is not so important because in the case of a small base length, which by simple theory would decrease the accuracy, the images of a stereo pair are more similar, improving the automatic image matching, so even with extreme base to height relation of 1:7 a system accuracy of 1.0 GSD for the height has been reached.

Table 4. Accuracy at independent check points

Images from	SX, SY	SZ [m]	GSD	SX,SY [GSD]	SZ [GSD]
SPOT -3	8.4	4.1	10 m	0.8	0.4
MOMS	3.5	4.5	4.5 m	0.8	0.4 / 0.13
Cartosat-1	1.5	2.5	2.5 m	0.6	0.7
IKONOS	1.0	1.7	1 m	1.0	0.2
ASTER	10.8	14.6	15 m	0.7	0.5
GeoEye-1	0.3	0.5	0.5 m	0.6	0.7
WorldView-2	0.5	0.3	0.5 m	1.0	0.2

As shown in table 4 the standard deviation for X, Y and Z of well defined points in a stereo model usually is slightly below 1.0 GSD. Of course this system accuracy is not identical to the accuracy of a DHM. At first with optical images as well as with SAR-images using X- and C-band DSM are generated and in addition areas with lower contrast and also terrain inclination and in the case of SAR fore-shortening and layover reduce the accuracy or even will lead to gaps in the data set. Nevertheless a major effect is the definition of the surface which has stronger effect for very high as for lower resolution images as it has been demonstrated above with LiDAR and aerial images. Very often DTM are requested which only can be generated by filtering and manual post-processing. The problems of accuracy specification can be seen also in table 5. If we compare a DHM based on WorldView-2 stereo pairs with another DHM based on a different WorldView-2 stereo model, the result is fitting better together as with other reference data because the surface definition of the both independent WorldView-2 DHM is similar – we have the same resolution, only the view direction is slightly different. So the standard deviation for flat areas is 0.66m. This is based on the comparison of two similar height models, so the standard deviation should be divided by 1.414 to get the standard deviation for a single DHM, leading to 47cm which is in the range of 1.0 GSD, but the NMAD which presents the frequency distribution usually better as the standard deviation, for flat areas is just 0.5m for the difference of both DHM. If we compare the WorldView-2 DHM with a reference DTM from the survey administration, we see larger discrepancies, also if we limit the investigated area to the open part, avoiding the influence of trees. In this case we can state, that the reference DTM is not as accurate as the WorldView-2 DHM. A comparison with LiDAR data avoids the problem of the accuracy of the reference data, but if we compare the data without taking care about the vegetation which has different influence in LiDAR DHM as in matched optical images, the discrepancies are large. Reduced to the open areas without quarries, which changed between imaging, the result becomes more realistic. For the flat part we now have a standard deviation of 0.83m or 0.71m NMAD which is still above the system accuracy of the DHM, but it should be respected, that the open area includes agriculture land where the vegetation changed between imaging.

Table 5. Accuracy analysis of WorldView-2 DSM Istanbul, absolute accuracy and as function of the terrain inclination with the slope α

	SZ	NMAD
WV-2 DSM against WV-2 DSM, open area	0.86m $0.66m+1.79*\tan\alpha$	0.69m $0.50m+1.29*\tan\alpha$
WV-2 DSM against reference DTM	3.65 m $3.25m+5.58m*\tan\alpha$	2.23 m $2.05m+5.17m*\tan\alpha$
WV2 DSM against reference DTM, open areas without quarries	2.21 m $1.85m+3.93m*\tan\alpha$	1.72 m $1.28m+3.24m*\tan\alpha$
WV-2 DSM against LiDAR DSM	3.12 m $3.12m+0.0*\tan\alpha$	1.40 m $1.40m+0.0*\tan\alpha$
WV-2 DSM against LiDAR DSM, open areas without quarries	1.05 m $0.83m+2.28*\tan\alpha$	0.71 m $0.62m+1.96*\tan\alpha$

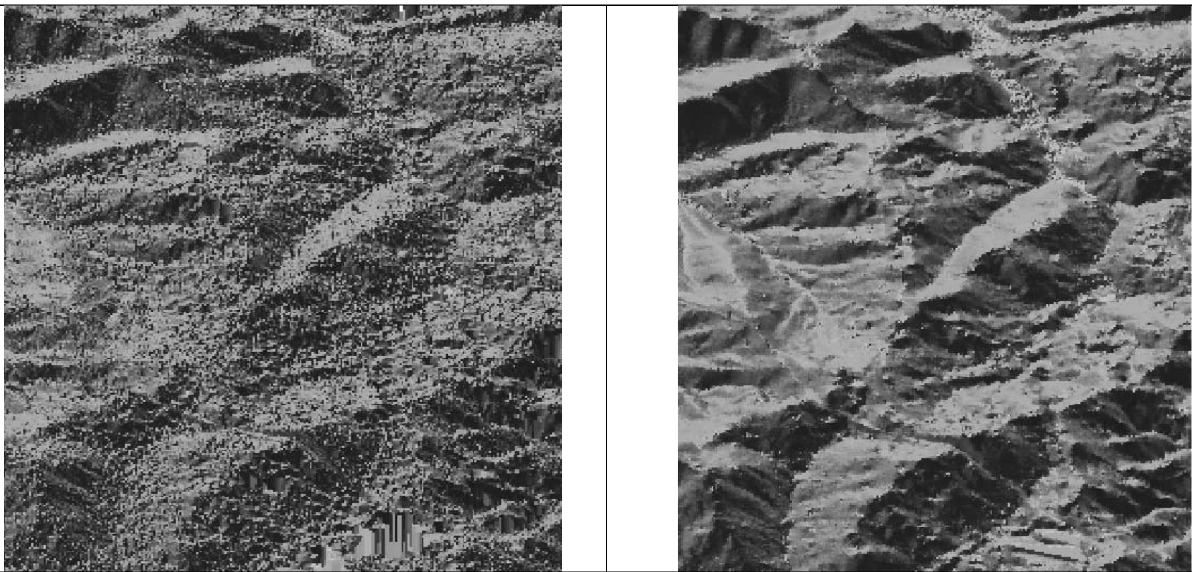

Original data | After filtering

Figure 7. 3D shaded view to WorldView-2 height model

The problem of the surface definition is obvious in figure 7, comparing the original DSM with a DTM generated by filtering. In the filtered image the main influence of the vegetation disappeared and the structure of the bare ground becomes clearer. This is a typical example for DHM from very high resolution space imagery. Also the dependency of the accuracy from the terrain inclination is usual for all DHM. With slightly lower resolution imagery as from Cartosat-1, Ziyuan-3, SPOT-5 HRS and ASTER the influence of the vegetation in relation to the accuracy is getting smaller. So for Cartosat-1 imagery with 2.5m GSD the system accuracy is in the range of a standard deviation of 2.5m, while the general accuracy is more in the range of 4m caused by lower contrast in some areas and the vegetation.

The fastest worldwide coverage with height models is possible with InSAR-configurations. The images for the SRTM C-band height model have been taken within 11 days in February 2000. For the clearly higher resolution and complete worldwide coverage the data acquisition for the TanDEM-X Global DEM takes approximately 2 years, but the whole world will be covered at least twice and the difficult areas with larger problems of foreshortening and layover will be covered a third and a fourth time with different base length and view direction. By the announced imaging time this will be done for approximately 20% of the area. The TanDEM-X Global DEM is specified with a relative standard deviation of SZ=1.2m within a sheet of 1° x 1°. The absolute accuracy shall be in the “meter range” (Eineder et al. 2013). This height model will have 0.4arcsec spacing, corresponding to 12m at the equator. In 2014 this will be the large area covering height model with the highest resolution and accuracy. Nevertheless the height models from the vhr optical images are more accurate and detailed, but they will not cover very large areas.

5. Conclusions

Height models may be generated with LiDAR for very high precision, with optical imagery and with SAR. SAR has problems especially in steep areas and cities while optical images have problems with low contrast. By this reason required gap fillings of SAR-DHM will be done with DHM from optical imagery and reverse. Even if we will have in near future the excellent TanDEM-X Global DEM, for details the optical imagery will have advantages with accuracy and resolution of course for higher cost. In addition the optical images have an additional advantage for mapping purposes beside use just for DHM generation. Aerial and space imagery do have for 0.5m up to 1m GSD an overlapping range where the use of the image type just depends upon the economic situation and the access to the imagery. In this overlapping range there is no special advantage of the space against the aerial images and reverse.

Acknowledgements

Thanks are going to Dr. Ricardo Passini, BAE Systems GP&S, NJ, USA, and Dr. Gürcan Büyüksalih, BIMTAS, Istanbul, for the support.

References

[1] Day, D., Jacobsen, K., Passini, R. & Quillen, S., 2013: *A Study on Accuracy and Fidelity of Terrain Reconstruction after Filtering DSMs produced by Aerial Images and Airborne LiDAR Surveys*, ASPRS Annual Convention Baltimore 2013

[2] Passini, R., Betzner, D., Jacobsen, K., 2002: *Filtering of Digital Elevation Models*, ASPRS annual convention, Washington 2002

[3] Eineder, M., Bamler, R., Cong, X., Gernhardt, S., Fritz, T., Zhu, X., Balss, U., Breit, H., Adam, N. & Floricioiu, D., 2013: *Globale Kartierung und lokale Deformationsmessungen mit den Satelliten TerraSAR-X und TanDEM-X,* Zeitschrift für Vermessungswesen 1/2013, pp75-94